

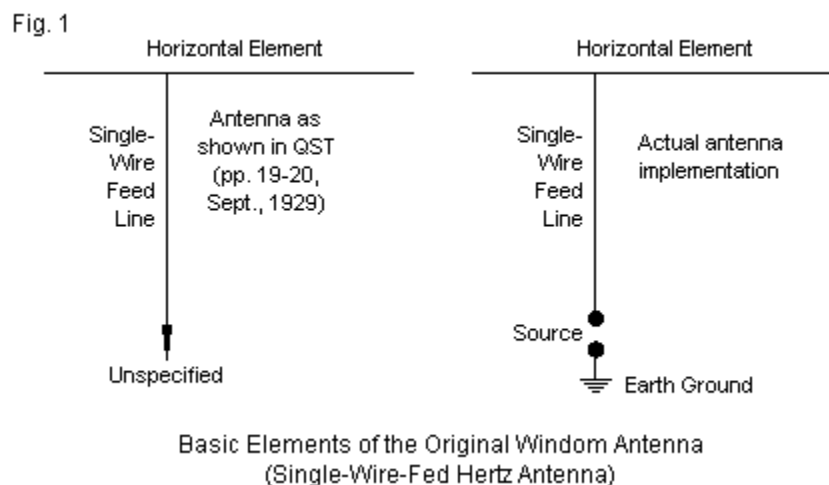
## Notes of Mr. Windom's "Ethereal Adornments"

L. B. Cebik, W4RNL

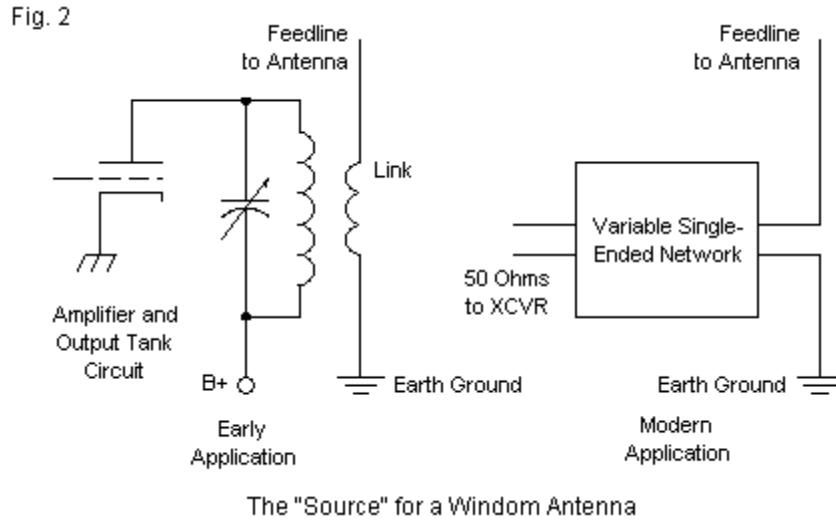
In the September, 1929, issue of *QST* (pp. 19-22, 84), Loren G. Windom, W8GZ-W8ZG, presented some interesting information in "Notes on Ethereal Adornments: Practical Design Data for the Single-Wire-Fed Hertz Antenna." The data resulted from his participation in a team of investigators at the Ohio State University under the direction of William L. Everitt. Although information was also published in the *Proceedings of the IRE* in October of the same year, the *QST* article has remained the key accessible source for the basic concept of the antenna that eventually came to bear Windom's name. However, as Windom told the story, "The writer acts solely as a reporter and all credit is due" to a long list of individuals named in the same paragraph. Had another of the group penned the *QST* article, the antenna would have a different name.

A Hertz antenna, as investigators used the term in that era, referred to any horizontal antenna that was not dependent upon the ground conditions for its performance. (In contrast, an antenna that depended upon the ground conditions and the antenna's connections to it bore the label "Marconi.") As we shall see, that is one misunderstanding of the antenna among several, since the ground plays a critical role in the operation of a Windom aerial.

The key to the Windom antenna is the use of a single-wire feeder with a calculated impedance of about  $500\ \Omega$ . Since the center point impedance of a half-wavelength horizontal wire is close to  $70\ \Omega$ , give or take about  $15\ \Omega$  depending upon antenna height, the single wire feeder required an offset feedpoint to provide what we would today call a match. **Fig. 1** presents the general appearance of the antenna in two forms.

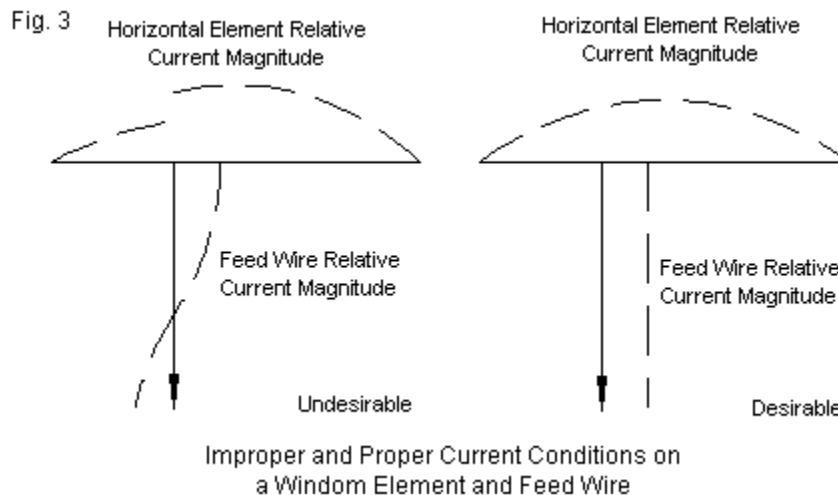


The form on the left shows the antenna as it appears in the article. The arrow replicates the original sketches, which do not specify a termination or source. The version on the right completes the antenna with a set of source-connection terminals and a mandatory earth ground connection. How users connected equipment to the antenna in 1929 differs from practice in the 21<sup>st</sup> century. **Fig. 2** provides sample connections. On the right, we find the typical modern variable network (in any of several configurations) that we might use to match the single-wire feeder impedance to a contemporary transceiver.



On the left is a situation—one variation among many—that represents the fairly standard 1929 connection. From the final transmitting tube to the antenna is a path through a resonant parallel tank circuit with a link coil to match the tank coil impedance to the antenna feeder impedance. Both versions of the connection show the requisite earth-ground connection.

Windom acknowledged that he and the Ohio State team were not the first to experiment with the single-wire-fed Hertz antenna, and he cited articles in *QST* for both 1925 and 1926 that presented earlier work. The new work focused upon the revised measurement techniques, using RF ammeters, to determine the proper connection point for the single-wire feeder. By ingenious and relatively simple methods, the team developed a means to ensure that the feeder attached at a point along the wire that allowed it to function as a feeder rather than as a part of the antenna itself.



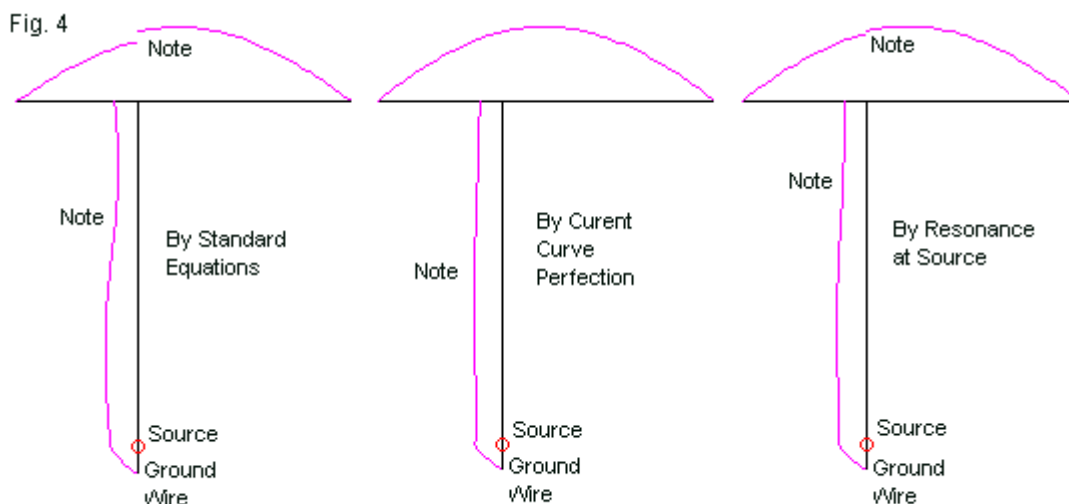
The left portion of **Fig. 3** shows an undesirable but common condition of early measurements that attempted simply to maximize current on the horizontal wire. The result tended to have two unwanted consequences. First, the current magnitude showed a disruptive step at the junction with the feed wire. Second, the feeder displayed standing current magnitude waves, contrary to its feedline function. The contrasting situation on the right, found

by measuring equal current magnitudes on each side of the feed-wire junction, resulted in a smooth near-sine-wave current magnitude pattern along the horizontal wire. As well, the current magnitude on the fed wire was virtually constant along its length.

Windom devoted the second half of his article to practical information for amateurs wishing to replicate the off-center-fed antenna. Using AWG #14 wire (0.0641" or 1.62 mm diameter) copper wire, Windom specified that the horizontal wire should be about  $0.483 \lambda$  (or,  $\lambda_{\text{meters}} = 2.07 L_{\text{meters}}$ ). The distance from the wire's center to the feedpoint connection as a fraction of the total horizontal wire length (L) is  $(L * 25)/180$ . The reason for the somewhat complex formula is that for much thinner wire, such as AWG #24, the numerator value grows from 25 to 30. We shall use AWG #14 copper wire throughout these notes, and so the feeder-placement formula simplifies to  $L * 0.14$  or 14% of wire length from its center point. As we measure such off-center-fed antennas today from the end, the feeder placement point is 36% of the distance along the horizontal wire.

The key to these notes lies in the NEC-4 models that we may create for the Windom antenna as originally presented. For any height above ground, we may model the horizontal wire as two wires, and place the vertical feed wire at the junction. The source for the antenna conventionally goes on the last segment of the feeder wire above ground. Because the antenna requires a definitive ground connection, I attached a 3-m wire from ground level straight downward to simulate a typical long ground rod or wire. There is no evidence that early versions of the antenna used any more complex form of ground treatment. For test models, I used 3.6 MHz as the design frequency, which resulted in a total length of 40.23 m (132.0'). The feeder length is simply equal to the height of the antenna above ground.

Horizontal antennas, such as center-fed dipoles, show some interesting properties at heights below  $2 \lambda$ . For example, their resonant length tends to vary with height in a cyclical fashion. So too does the resonant center point feed impedance. Since the Windom is by initial declaration a Hertz antenna, it should reflect similar properties, adjusted for the off-center feed-wire junction. In the end, for each antenna height, we wind up with three related but different models of the antenna, as shown in **Fig. 4**.



Three Ways of Modeling a Windom Single-Feed-Wire Hertz Antenna

The first version models the antenna according to the basic equation. Hence, the two sides of the horizontal element have invariant lengths: 14.48 m and 25.75 m. As the current magnitude curves show, the element curve has an unwanted step, and the feeder wire shows a standing wave. We may adjust the length of one of the horizontal wires to perfect the current curve and remove the step at the feed-wire junction, as shown by the middle outline. The feeder current curve is nearly a straight line, indicating the attenuation of the standing wave. However, the resulting source impedance is not resonant. Therefore, we may make further horizontal-wire adjustments to arrive at a resonant impedance. As the sketch on the right shows, the standing wave reappears on the feeder. As well, a step reappears in the current curve, and its size depends upon the height of the antenna and the resulting length of the feeder wire. Ultimately, we shall use the current-perfect version of the antenna at all heights for further exploration, but initially, we shall work with all three types of models.

The screenshot shows the 'Wires' window in EZNEC software. The title bar reads 'Wires'. The menu bar includes 'Wire', 'Create', 'Edit', and 'Other'. The main title is 'Typical EZNEC Model Used to Evaluate Windom Performance' with 'Fig. 5' in the top right. Below the title bar are several checkboxes: 'Coord Entry Mode' (unchecked), 'Preserve Connections' (unchecked), 'Resonant Version at 0.5 wl above Ground' (checked), and 'Show Wire Insulation' (unchecked). The main area contains a table with the following data:

Wires											
No.	End 1				End 2				Diameter (mm)	Segs	
	X (m)	Y (m)	Z (m)	Conn	X (m)	Y (m)	Z (m)	Conn			
1	-15	0	41.64		0	0	41.64	W2E1	#14	29	
2	0	0	41.64	W3E1	25.75	0	41.64		#14	51	
3	0	0	41.64	W1E2	0	0	0	W4E1	#14	83	
4	0	0	0	W3E2	0	0	-3		#14	6	
*											

**Fig. 5** shows the wire table for a typical NEC-4 model using EZNEC, v.5. The model shown happens to be the resonant version of Windom with a  $0.5 \lambda$  feeder wire (since a wavelength at 3.6 MHz is 83.2757 m). All dimensions in these notes are metric as a matter of modeling convenience. My strategy for adjusting the antenna from its initial versions derived from the 1929 equation (called Eq) was to shorten or lengthen the shorter of the two wires until achieving a virtually perfect current magnitude curve (called Cur). (The currents on each of the three wires at the junction also show interesting phase-angle differences, but since the 1929 measurements only recorded current magnitude, we may restrict our present interest to just those values.) Moving from the initial Eq version to a resonant version (called Res) allowed adjustment of the same shorter wire at most heights, but at two heights, no resonance resulted. In those cases, I adjusted the length of the longer wire. The relatively high impedance of the feedpoint junction required close attention to maintaining the same segment length for all segments in the model. The target value was 0.5 m throughout.

The survey of possible Windom antennas placed the horizontal wire at heights above average ground (conductivity 0.005 S/m, permittivity 13) at  $0.125 \lambda$  intervals from  $0.125 \lambda$  to  $1.0 \lambda$ . For each height, we find 3 models—one of each type—along with their dimensions, feedpoint impedance values, junction current magnitude values, and the performance data. The results appear in **Table 1**. Due to the quantity of the data, the table appears in two tiers. The performance data includes, besides the usual maximum gain in dBi and the take-off (TO) angle (the elevation angle of maximum gain), a third figure showing the azimuth heading of maximum gain, where a value of  $90^\circ$  is broadside to the horizontal wire itself. The goal of the data collection is to allow relatively easy comparison of the conditions that emerge from developing at each height the equation-based model, the perfected-current model, and the model having a resonant feedpoint impedance.

Original Windom Antenna from QST, September, 1929											Table 1	
Data from NEC-4 Models at 3.6 MHz in 1/8-wl increments											Wire: AWG #14 (0.0641" = 1.63 mm diameter)	
All lengths in meters (divide by 0.3048 for lengths in feet)											1 wl = 83.2757 m; Lttl (Eq) = 0.483 wl	
Model versions: equation (Eq), current curve (Cur), resonance (Res)												
Models bring single feedline to ground with a 3-m vertical wire into ground												
Horizontal wires: Lsh = short end, Llng = long end, Lttl = total horizontal length; Pos = percent from short end												
Vertical wire: Lfd = vertical wire from horizontal down to ground (= height)												
Currents: Ish, Ilng, Ild-junct = currents on short, long, and feed wires at junction												
Ild-min, Ild-max = minimum and maximum current magnituds on feedline wire												
FPZ = feedpoint impedance: resistive and reactive in Ohms												
Az angle: 90 deg. = broadside to horizontal wire; TO angle = elevation angle of maximum gain (in dBi)												
Ht wl	Ht m	Version	Lttl	Lsh	Llng	Pos. (%)	FPZ-res	FPZ-react				
0.125	10.41	Eq	40.23	14.48	25.75	36.0	502.4	-358.5				
		Cur	40.23	14.48	25.75	36.0	502.4	-358.5				
		Res	41.68	15.93	25.75	38.2	287.3	0.5				
0.25	20.82	Eq	40.23	14.48	25.75	36.0	549.0	-86.3				
		Cur	40.25	14.50	25.75	36.0	550.9	-81.8				
		Res	40.60	14.85	25.75	36.6	588.2	0.0				
0.375	31.23	Eq	40.23	14.48	25.75	36.0	497.8	63.6				
		Cur	40.80	15.05	25.75	36.9	611.4	-98.5				
		Res	40.95	14.48	26.47	35.4	632.8	-0.4				
0.5	41.64	Eq	40.23	14.48	25.75	36.0	681.7	155.7				
		Cur	40.95	15.20	25.75	37.1	693.4	-64.7				
		Res	40.75	15.00	25.75	36.8	707.6	0.4				
0.625	52.05	Eq	40.23	14.48	25.75	36.0	738.1	-267.0				
		Cur	40.65	14.90	25.75	36.7	610.2	-204.6				
		Res	41.77	16.02	25.75	38.4	392.4	0.8				
0.75	62.46	Eq	40.23	14.48	25.75	36.0	543.4	-143.5				
		Cur	40.53	14.78	25.75	36.5	568.2	-78.5				
		Res	40.87	15.12	25.75	37.0	603.5	0.9				
0.875	72.87	Eq	40.23	14.48	25.75	36.0	514.7	-46.0				
		Cur	40.75	15.00	25.75	36.8	621.5	-72.9				
		Res	40.78	14.48	26.30	35.5	616.1	0.8				
1	82.28	Eq	40.23	14.48	25.75	36.0	672.2	92.8				
		Cur	40.90	15.15	25.75	37.0	661.0	-86.9				
		Res	40.58	14.83	25.75	36.5	683.5	0.8				
Ht wl	Ht m	Version	Ish	Ilng	Ild-junct	Ild-min	Ild-max	Imax-min	Max gain	Az angle	TO angle	
0.125	10.41	Eq	2.555	2.547	0.608	0.569	1.000	0.431	5.10	134	86	
		Cur	2.555	2.547	0.608	0.569	1.000	0.431	5.10	134	86	
		Res	2.070	1.469	0.796	0.796	1.000	0.204	4.12	170	87	
0.25	20.82	Eq	2.355	2.066	0.948	0.948	1.097	0.149	5.08	96	59	
		Cur	2.038	2.084	0.772	0.772	1.000	0.228	5.08	96	59	
		Res	2.188	2.076	0.840	0.840	1.000	0.160	5.03	96	59	
0.375	31.23	Eq	1.750	2.022	0.779	0.689	1.000	0.311	5.27	91	37	
		Cur	2.110	2.166	0.892	0.892	1.000	0.108	5.37	92	37	
		Res	2.091	2.110	0.806	0.806	1.013	0.207	5.30	90	37	
0.5	41.64	Eq	2.205	2.623	0.836	0.696	1.195	0.499	6.43	89	28	
		Cur	2.495	2.552	0.847	0.847	1.036	0.189	6.57	89	27	
		Res	2.446	2.612	0.838	0.826	1.090	0.264	6.55	89	28	
0.625	52.05	Eq	2.493	2.773	0.793	0.750	1.219	0.469	6.92	89	22	
		Cur	2.384	2.426	0.727	0.727	1.022	0.295	6.86	88	22	
		Res	2.081	1.623	0.810	0.487	1.000	0.513	6.32	89	23	
0.75	62.46	Eq	1.951	2.124	0.714	0.698	1.000	0.302	6.07	89	19	
		Cur	2.062	2.108	0.742	0.742	1.000	0.258	6.03	88	19	
		Res	2.201	2.087	0.808	0.787	1.000	0.213	5.97	88	19	
0.875	72.87	Eq	1.774	2.025	0.728	0.662	1.000	0.338	5.73	90	16	
		Cur	2.100	2.148	0.823	0.823	1.000	0.177	5.82	91	16	
		Res	2.012	2.075	0.739	0.739	1.003	0.264	5.72	90	16	
1	82.28	Eq	2.087	2.433	0.799	0.698	1.127	0.429	6.07	91	14	
		Cur	2.296	2.322	0.814	0.814	1.000	0.186	6.24	92	14	
		Res	2.223	2.410	0.800	0.779	1.056	0.277	6.17	90	14	

Perhaps the first comparison to make is within each group of models for each height. The correct increment between  $I_{sh}$  and  $I_{lng}$  is between 0.00 and 0.08, with an optimum value of about

0.04. (The source current in all cases is 1.000 and all modeled current values are relative to this value.) At every height except the lowest, there is a significant difference between the Eq values and the Cur values for total element length, junction position, and maximum gain. The table also records the minimum and maximum current values on the feeder wire. The difference between these values is least almost (but not quite) universally with the Cur version of the antenna. Equally, the antenna almost always shows maximum gain with the Cur version.

Readjusting the antenna for a resonant feedpoint impedance does not improve performance by changing the antenna dimensions to achieve this goal. In virtually all cases, the gain decreases and a current step emerges at the junction with the feed wire. As well, the variation in relative current magnitude increases on the feed wire, indicating a larger standing wave. The conditions that Windom and the Ohio State University group set for optimal operation of the single-wire-fed Hertz antenna—a smooth current progression on the horizontal wire and minimum current magnitude variation on the feed wire—turn out to be the conditions for best modeled antenna performance using the 3 meter ground wire.

As we change our perspective to move from one height to the next within any one of the model versions, we find that the antenna dimensions and the feed-wire junction position change from one height to the next. We may examine some of these changes in comparison with corresponding changes for a resonant center-fed dipole for the same band. For the Windom, we shall use the Cur version and look at the total length and the feed-wire junction position in comparison with the resonant length of the dipole at each surveyed height. As well, we may compare the maximum gain of each antenna at each height. **Table 2** provides the numerical data. Our goal is not to evaluate relative performance between the antennas but to explore the progression of values.

Behavior Parallels: Windom vs. Resonant Dipole at the Same Heights							Table 2	
Windom = Current Curve Perfected Version; Dipole = Center-Fed Resonant Wire								
Ht wl	Ht m	Windom Lttl-m	Windom Lttl-wl	Res Dpl L-wl	Windom Pos %	Windom Gain dBi	Res Dpl Gain dBi	
0.125	10.41	40.23	0.4831	0.4802	36.0	5.10	5.89	
0.25	20.82	40.25	0.4833	0.4823	36.0	5.08	6.17	
0.375	31.23	40.80	0.4899	0.4895	36.9	5.37	6.45	
0.5	41.64	40.95	<b>0.4917</b>	<b>0.4923</b>	<b>37.1</b>	6.57	7.73	
0.625	52.05	40.65	0.4881	0.4858	36.7	<b>6.86</b>	<b>8.14</b>	
0.75	62.46	40.53	0.4867	0.4848	36.5	6.03	7.44	
0.875	72.87	40.75	0.4893	0.4878	36.8	5.82	7.28	
1	82.28	40.90	<b>0.4911</b>	<b>0.4888</b>	<b>37.0</b>	6.24	7.85	
Notes:	1. Peak values = boldface-italics							
	2. Minimum values = italics							

The table indicates peak values in boldface italics and minimum values in italics. The coincidence of peak and minimum dimensional values is striking. In both cases, gain maximums and minimums do not occur at the same heights as maximum and minimum antenna lengths. As well, both types of antennas appear to show similar curves such that the difference between maximum and minimum values decreases as we increase the antenna height. **Fig. 6** graphs the element lengths and the Windom feed wire junction position, while **Fig. 7** graphs the maximum gain progression for each antenna. Except at the lowest height ( $1/8 \lambda$  or 10.41 m or 34.2'), the parallels are sufficiently exact to suggest that the Windom responds to the ground just as does a standard dipole. For these comparisons, both antennas are above average ground quality.

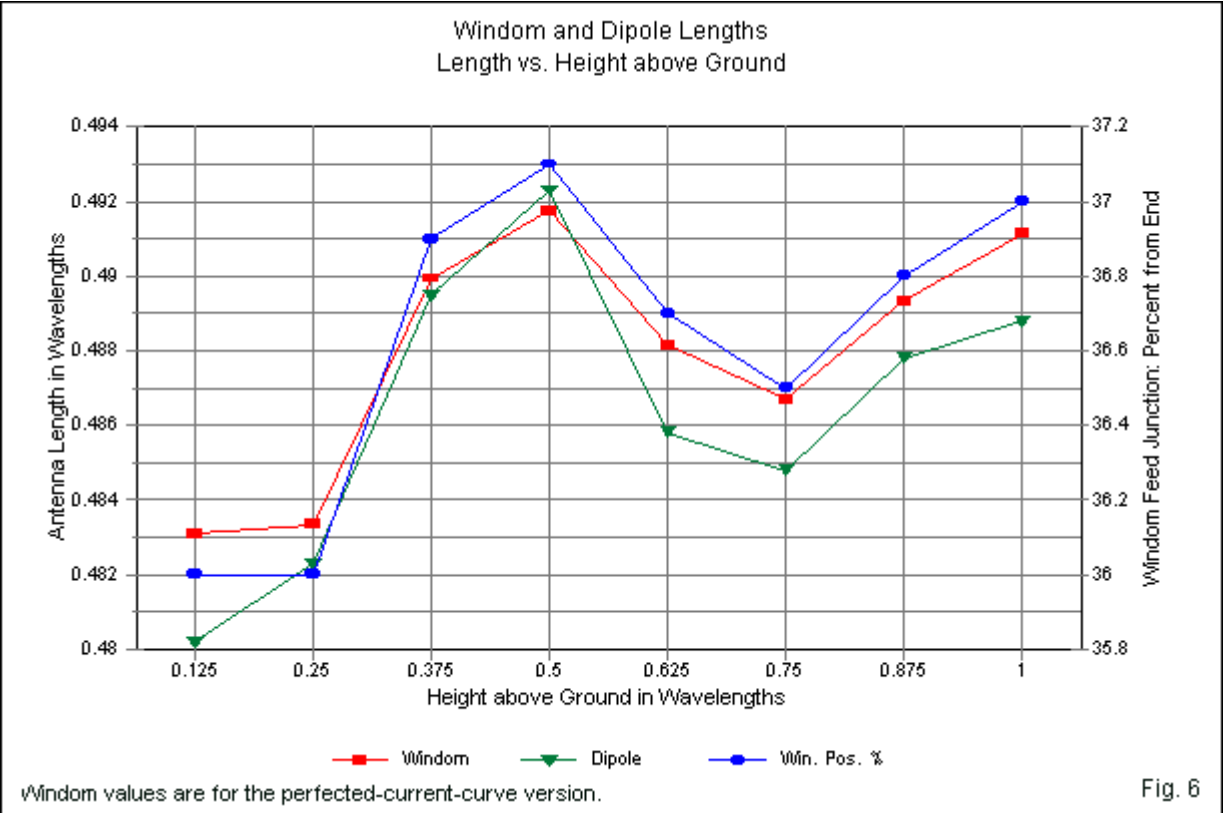


Fig. 6

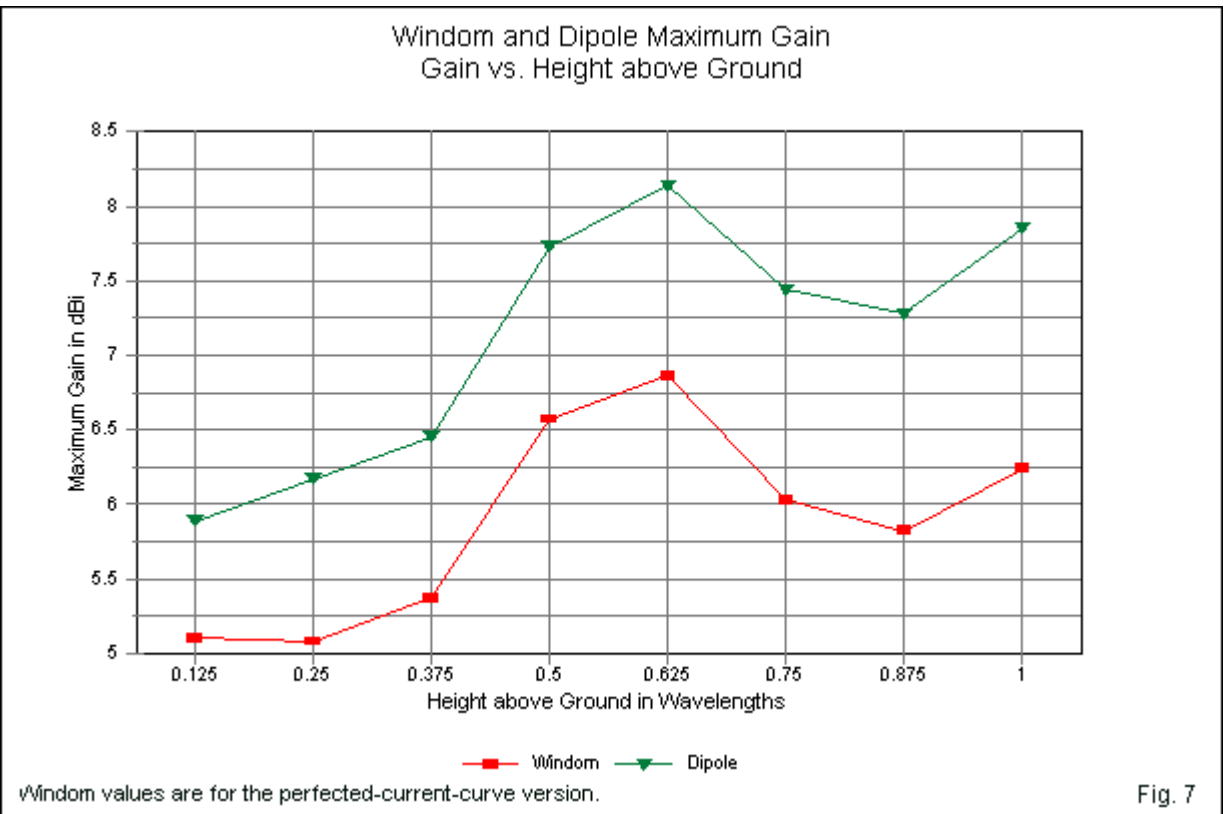
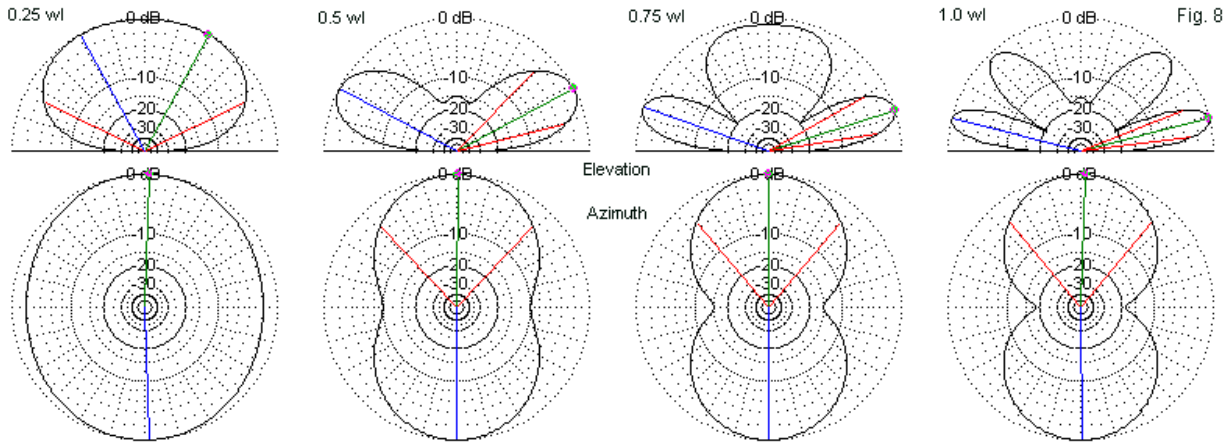


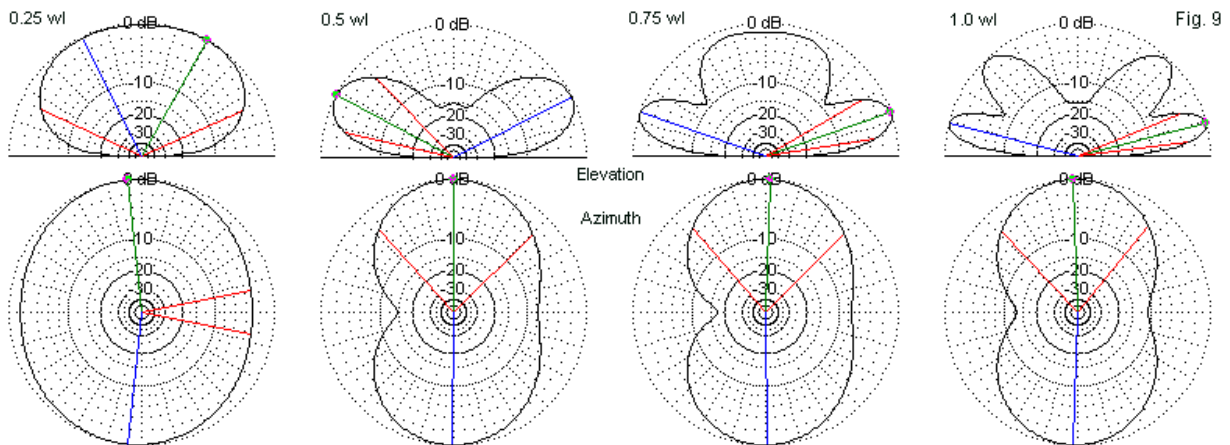
Fig. 7

The parallel results between an original Windom and a dipole do not indicate that the two antennas provide the same patterns at each height. **Fig. 8** supplies elevation and azimuth patterns for the resonant dipole at different heights in  $0.25 \lambda$  increments. In all cases, the elevation pattern uses a heading that is exactly broadside to the dipole wire. The evolution of the patterns from a broad oval at the lowest height to nearly a figure-8 at the highest level is readily apparent.



Note: Elevation patterns are along the main axis of the strongest lobes, which are broadside to the wire.

Elevation and Azimuth Patterns of a Resonant Dipole at 3.6 MHz at Selected Heights above Average Ground



Note: Elevation patterns are along the main axis of the strongest lobes, which are broadside to the horizontal wire. Left side of the azimuth pattern corresponds to the short end of the horizontal wire.

Elevation and Azimuth Patterns of a Current-Perfect Windom at 3.6 MHz at Selected Heights above Average Ground

Corresponding elevation and azimuth patterns for the current-perfected Windoms appear in **Fig. 9**. At each height, the heading for maximum gain is different and rarely is exactly broadside to the horizontal wire. As well, the azimuth patterns show an offset that varies with height. At  $0.25 \lambda$ , the radiation off the short end of the Windom is stronger than off the long end. This pattern reverses by a height of  $0.5 \lambda$ . However, the difference decreases at  $1 \lambda$  suggesting that the relative strength of radiation off the ends might undergo a cycle of its own.

The current magnitude curves that we have examined and to which the Everitt group restricted itself give no clue as to the shifting azimuth patterns or to variations that we find in the

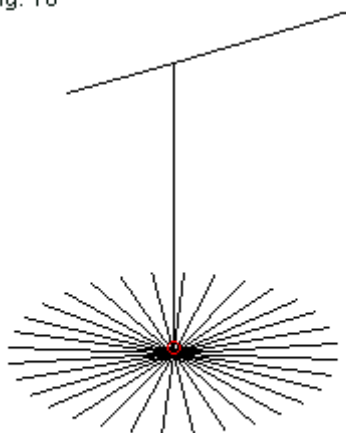


upper elevation lobes above  $0.5 \lambda$ . Examining current magnitude alone yields curves identical in shape to those produced by dipoles. However, the phase angle of the current undergoes a sudden shift at the junction with the feed wire. The phase angle changes by about  $20^\circ$ , with the long end showing a more positive phase angle. In addition, the current along the feed wire at the junction is about  $1/3$  the value of the current on the horizontal wire. Although the horizontal wire may dominate in the formation of the Windom radiation patterns, the unconfined fields from the feeder wire are sufficient to modify those patterns from the symmetrical arrangements that mark the standard center-fed dipole.

The data that the models produce was not accessible to the investigators who developed the original Windom arrangement. Moreover, it is likely that most of the experiments employed horizontal wires for either 80 or 40 meters at fairly low heights. However, they did note the ability to scale the antenna for any HF frequency. Hence, our exploration of greater heights as fractions of a wavelength is certainly in order. So too are certain supplementary analyses of Windom behavior. For example, if we omit a ground connection and try to feed the antenna on the lowest segment above a feeder that does not reach ground, we obtain a wholly unusable impedance. The resistive component—depending upon antenna height and the resulting feeder length—can reach values that double the values listed in **Table 1**, while the reactive component can in some cases exceed  $20,000 \Omega$ .

Although there is no evidence that the Windom experiments used a buried ground radial system similar to one that we might apply to a vertical monopole, we may easily model such a system. As an exercise, I replaced the simple 3 m ground wires with a system of  $1/4 \lambda$  radials buried 0.5 m below ground for the 3.6 MHz Windom. I created such systems for current-perfected version of the antenna for antenna heights of  $1/4$ ,  $1/2$ ,  $3/4$ , and  $1 \lambda$ . **Fig. 10** shows the general outline of the models with a  $0.5 \lambda$  feeder. The goal was to determine if improving local ground conditions would improve antenna performance in any way, especially in view of the fact that the single-wire feeder contributes to the overall radiation pattern of the antenna, even if not in a dominant way. As the figure shows, the models used 32 radials, an intermediate size field between simple amateur 4-wire fields and commercial 120-radial fields.

Fig. 10



Outline of a Windom  
with 32  $1/4$ -WL Radials

The results of the experimental models appear in **Table 3**.

A Comparison of Standard and Improved Ground Conditions for Current-Perfectd Windom Models						Table 3
Ground-Wire Only						
Ht wl	Ht m	Max gain	Az angle	TO angle	FPZ-res	FPZ-react
0.25	20.82	5.08	96	59	550.9	-81.8
0.5	41.64	6.57	89	27	693.4	-64.7
0.75	62.46	6.03	88	19	568.2	-78.5
1	82.28	6.24	92	14	661.0	-86.9
32 Buried 1/4 WL Radials						
Ht wl	Ht m	Max gain	Az angle	TO angle	FPZ-res	FPZ-react
0.25	20.82	5.85	96	60	483.3	-47.1
0.5	41.64	7.14	89	28	622.2	-33.7
0.75	62.46	6.68	89	19	496.6	-52.1
1	82.28	6.77	91	14	591.3	-61.6
Differences (Radial Field Values - Ground Wire Values)						
Ht wl	Ht m	Max gain	Az angle	TO angle	FPZ-res	FPZ-react
0.25	20.82	0.77	0	1	-67.6	34.7
0.5	41.64	0.57	0	1	-71.2	31.0
0.75	62.46	0.65	1	0	-71.6	26.4
1	82.28	0.53	-1	0	-69.7	25.3
Notes: See Table 1 for explanations of column heading labels.						

The addition of a significant buried radial field shows performance improvements and other notable trends for the current-perfected Windom model. The average gain improvement with the radials is about 0.6 dB, an amount that is more numerically noticeable than operationally detectable. The key angular values that apply to the patterns show no significant change and the patterns themselves are virtually identical to the ones shown in **Fig. 9**. The improved local ground reduces the resistive component of the feedpoint impedance by about 70  $\Omega$  or about 11%. As well, the capacitive reactance shows a considerable reduction, bringing the feedpoint closer to resonance with an SWR referenced to the resistive component well below 1.5:1.

A local ground modification—here in the form of 32 buried radials—improves the antenna performance by increasing its efficiency, that is, by reducing the resistive losses at the source connection. We may also check the effect of different ground qualities on performance as they apply both to the immediate installation and to the far field. To this end, I placed the current-perfected model of the Windom, with a height and feeder length of  $0.5 \lambda$ , over very good, average, and very poor soil. Since this exercise has a counterpart exercise with resonant dipoles, I examined the same ground quality range with a dipole  $0.5 \lambda$  above ground. In both cases, I used antennas that we have previously examined over average soil alone.

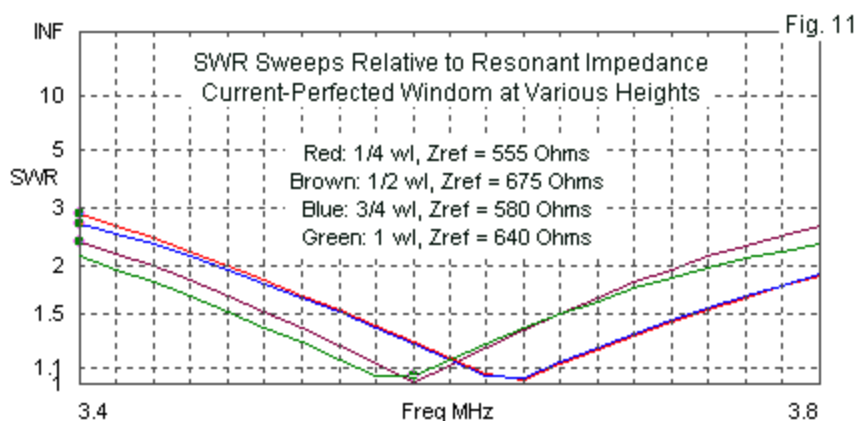
**Table 4** shows the results of the exercise. Within the group of Windom models, the current data is significant. If we use the version over average ground as a standard, then the current increment between the short and long ends of the wire at the junction with the feed wire deviates from the standard as we change the ground quality. The increment over average ground is about 0.05, but over very poor ground, there is no difference in value. Over very good ground the increment increases to about 0.10. Although the deviations are relatively small, they do indicate that the overall ground quality can affect the horizontal wire current curve.

When we compare the Windom to the dipole, we discover that ground quality has a much more profound affect on the performance of the single-wire-fed Hertz antenna. The gain of the Windom undergoes twice the variation of the dipole gain. The dipole feedpoint resistance changes by about 2%, while the feedpoint resistance of the Windom changes by about 23%.

Even greater is the radical change in the Windom's feedpoint reactance, especially when compared to the 8 Ω change in the dipole's reactance over the same range of ground qualities.

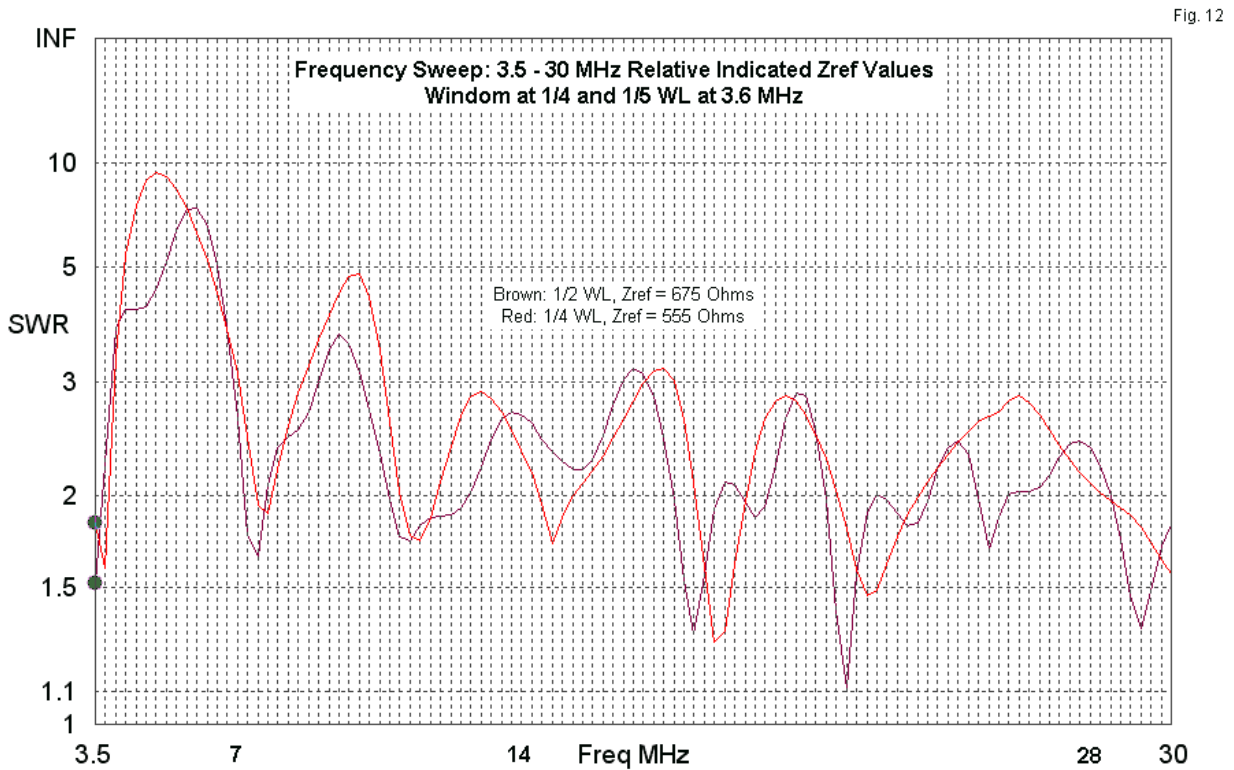
A Comparison of Windom vs. Dipole Performance over Various Ground Qualities								Table 4
Antenna height: 1/2 WL (41.64 m) above ground								
Windom (current-perfected model with a 3 m ground wire)								
Ground	Max gain	Az angle	TO angle	FPZ-res	FPZ-react	Ish	lIng	lfd-junct
Very Gd	7.30	89	28	645.0	-15.0	2.477	2.575	0.854
Average	6.58	89	27	693.4	-64.7	2.495	2.552	0.847
Very Pr	5.05	90	27	810.7	-280.4	2.467	2.468	0.837
Diff.	2.25			165.7	265.4			
Dipole (resonant over average ground)								
Ground	Max gain	Az angle	TO angle	FPZ-res	FPZ-react			
Very Gd	8.12	90	29	68.4	-3.3			
Average	7.73	90	28	68.6	0.0			
Very Pr	7.01	90	26	69.9	4.3			
Diff.	1.11			1.5	-7.6			
Ground Quality Values:								
	Very Good: conductivity 0.0303 S/m, permittivity 20							
	Average: conductivity 0.005 S/m, permittivity 13							
	Very Poor: conductivity 0.001 S/m, permittivity 5							

Nevertheless, we should not interpret these results as suggesting that the current-perfected Windom model is has a very narrow operating bandwidth. A wire dipole has a 2:1 SWR bandwidth relative to its resonant impedance of about 200 kHz. **Fig. 11** tracks the SWR values relative to the resistive component of the feedpoint impedance at heights of 1/4, 1/2, 3/4, and 1 λ. Because the reactive component varies in each case, the resonant frequencies do not neatly align with each other. Still, the average 2:1 SWR bandwidth is about 350 kHz. In addition, the output tuning networks used in 1929 were virtually all variable and capable of handling wider ranges of impedance than today's fixed component networks. Hence, coverage of the entire 80-75-meter band was feasible. The test frequency of 3.6 MHz limits the model's ability to show the full SWR curve.

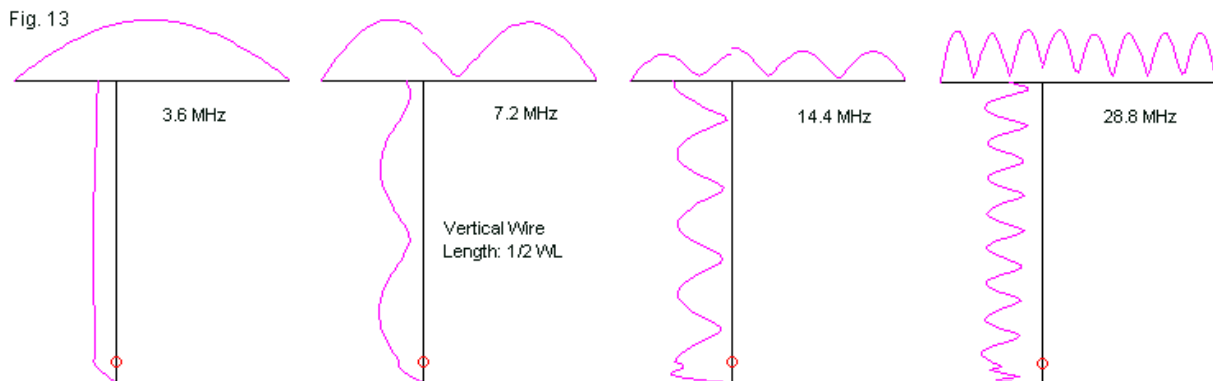


Interestingly, the original Windom article refers to use of the antenna on multiple harmonically related amateur bands, most notably for that era, 80, 40, 20, and 10 meters. The author specifically mentions successfully operating his version of the antenna at 28 MHz. We might therefore briefly examine this capability by several means. One usual method is to create

a broad SWR sweep across the HF region from 3.5 to 30 MHz. **Fig. 12** performs that task for versions of the Windom at heights of  $\frac{1}{4}$  and  $\frac{1}{2}$   $\lambda$ .



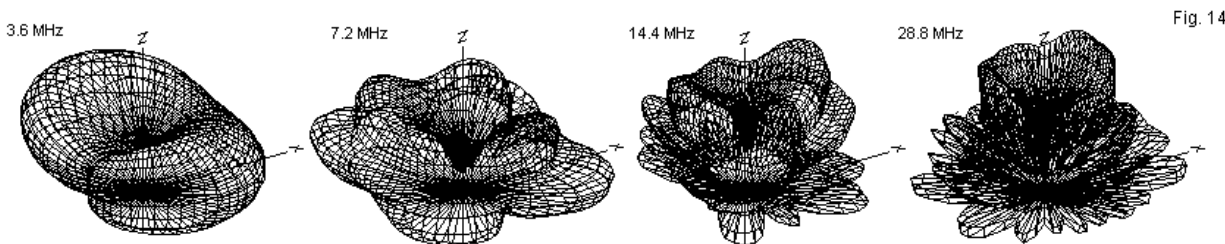
If we impose our present-day 2:1 SWR standard, then the antenna appears not to meet the need. If we expand the SWR limits to 3:1, the antenna shows at either height only a few lower-frequency regions outside the limit. (We should also remember that maximizing antenna current and not a low SWR was the general mark of a successfully loaded antenna in the late 1920s. Our SWR fetish emerged with the 1960s and the development of SSB transceivers with fixed output components, even with tube-type output amplifiers.) If the ability to obtain relatively high antenna currents was the author's mark of successful high-band antenna operation, then a Windom cut for a lower band would operate on a high harmonic band.



Current Magnitudes along the Wires of a Current-Perfect Windom at Its Fundamental and Harmonic Frequencies

**Fig. 13** shows the relative current magnitudes on the horizontal and feeder wires of the 3.6 MHz Windom on each of the available bands, using harmonics of the test frequency. On the fundamental frequency, the curves show the desired conditions of a smooth current curve on the horizontal wire and a feeder wire with virtually a constant current magnitude. However, as we raise the operating frequency, the required conditions disappear. The junction point between short and long ends of the horizontal wire shows a distinct step. (The 10-meter step is less visible because it occurs at a low region of the overall curve.) Perhaps more significant is the development of large standing waves on the feeder wire, indicating the potential for considerable radiation.

The current magnitude curves, even without reference to the current phase angles along the wires, do not bode well for harmonic operation of the original Windom in terms of the radiation patterns. Indeed, the patterns become so complex that standard elevation and azimuth pattern do not suffice above the second harmonic. The 80- and 40-meter patterns are reasonable normal, as the 3.6 MHz bi-directional pattern becomes a cloverleaf at 7.2 MHz. However, as the remaining patterns in **Fig. 14** reveal, the upper bands show predominantly high-angle radiation. As with most antennas, the user might obtain some contacts, but other antenna types would serve much better in providing the low-angle radiation necessary for consistent long distance communications.



3-Dimensional Patterns of the Current-Perfected Version of the Original Windom on Its Fundamental and Harmonic Frequencies

The original Windom, by modern evaluation, becomes essentially a monoband antenna. In that regard, it differs from other off-center-fed antennas that are more commonly used today. **Fig. 15** over-simplifies the field by reducing the major types to only three. The first is the original Windom with its single-wire feeder. The second uses a parallel transmission line in place of the single-wire feeder. The third uses various means of isolating the horizontal element from the feedline so that only balanced currents occur on the line. With each outline sketch is an inset showing the relevant current magnitude curves along the relevant wires for the second harmonic of the 3.6 MHz design frequency. All 3 samples use a 37% feedline placement.

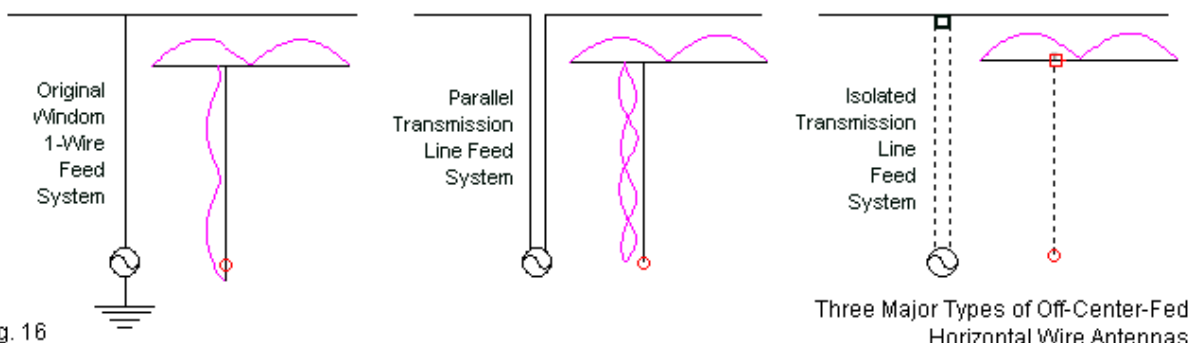
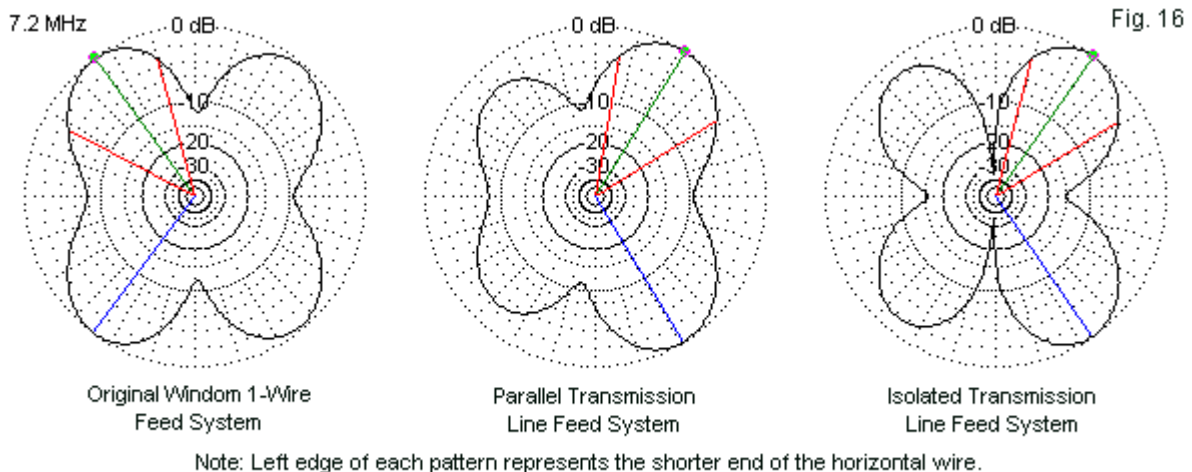


Fig. 16

Three Major Types of Off-Center-Fed Horizontal Wire Antennas

All three versions of the antenna show essentially the same horizontal wire current magnitude curves. The Windom reveals its high standing waves on the feeder. The fact that the parallel transmission line also shows current magnitude curves that differ for each of the two wires indicates that the feedlines have radiation currents as well as transmission line currents. Only in the last case, on the assumption that the designer has achieved effective feedline isolation from the offset connection point, do we find no radiation currents on the feedline.

The different forms of feeding the off-center-fed antennas have consequences for the second harmonic radiation pattern. **Fig. 16** shows the azimuth patterns for the antenna at a modeled height of  $\frac{1}{2} \lambda$  at the fundamental frequency. The elevation angle for all of the patterns is  $7^\circ$ .



Second Harmonic Azimuth Patterns for Three Types of Off-Center-Fed Horizontal Wire Antennas

The pattern on the right, which assumes a perfectly isolated feedline, presents the “purest” appearance, with deep nulls in the offset cloverleaf that is stronger toward the long end of the antenna. (In fact, this model has limited utility outside the present context, since upper-band patterns will vary according to the exact position of the feedpoint.) When we do not isolate the feedline but use parallel transmission line (usually to an antenna tuner), we encounter two difficulties. First, the radiation from the feedline reduces the pattern’s sharpness, not only reducing the depth of the pattern nulls, but also reducing the strength of the major lobes. The middle pattern has a maximum gain that is about 1 dB lower than the pattern on the right. The single-wire feeder system on the left appears to present a more symmetrical pattern, but at the cost of another dB of maximum gain.

The net result is a set of differences that simply establish that the original Windom is not the same as the types of off-center-fed (OCF) antennas used today. We may bypass modern OCFs, since the interests of these notes have been in the analysis of the 1929 Windom with its single wire feeder. The ethereal adornment that bears Windom’s name is a fascinating antenna to study, even if we have not the slightest interest in building one today. In fact, I know of no one who has a true Windom. Essentially, everything that today bears the label “Windom” isn’t.